Holistic Life Cycle Optimization of Building Energy Standards by balancing Heating and Cooling Loads

Jonatan Höpp[a,b], Nico Fuchs[a], Dirk Müller[a]

[a] *RWTH Aachen University, E.ON Energy Research Center, Institute for Energy Efficient Buildings and Indoor Climate, Aachen, Germany*
[b] *jonatan.hoepp@eonerc.rwth-aachen.de, CA*

Abstract:

The drive towards nearly zero-energy buildings through enhanced insulation and airtightness is a cornerstone of climate change mitigation in the building sector. However, this trend introduces a critical trade-off: reduced heating demand at the cost of significantly increased cooling requirements, a challenge intensified by future climate scenarios. This work investigates this heating-cooling trade-off to identify optimal building energy standards of a non-residential office building by holistically evaluating a detailed life cycle perspective of emissions and costs over a 40-year horizon. This paper builds upon a previously developed two-stage, automated, holistic optimization framework for non-residential buildings. Unlike previous holistic approaches that often neglect or simplify distribution networks, this methodology optimizes the building envelope, hydraulic and air distribution systems, and the building's energy hub with high granularity. It employs Mixed-Integer Linear Programming (MILP) formulation for design and operational optimization of the energy hub and simultaneously conducts rigorous economic and ecological life cycle assessments rather than solely optimizing for costs or emissions. Key enhancements include thermal comfort assurance across design variants, integration of dynamic shading systems, and expansion to international building energy standards. The energy hub optimization focuses exclusively on renewable, electrified technologies. The application of the method to a non-residential office building in Aachen, Germany, reveals that the highest insulation standards are not necessarily optimal from a life cycle perspective. Optimal building energy standards emerge at moderate insulation levels with opaque envelope U-values between 0.2 to $0.25\,\mathrm{W\,m^{-2}\,K^{-1}}$, combined with concrete core activation systems. At these standards, moderate insulation balances envelope embodied impacts against heating-driven operational energy reductions, while peak cooling load constraints prevent corresponding reductions in Heating, Ventilation and Air Conditioning (HVAC) system embodied impacts. The findings demonstrate that, under the assumed boundary conditions, an over-emphasis on envelope insulation paradoxically leads to carbon-intensive HVAC infrastructure scaled by peak loads, offsetting envelope-driven operational benefits and degrading overall life cycle performance compared to moderate insulation strategies. As this analysis is bounded to a building in a temperate climate with high-performance passive cooling systems, results are not generalizable to tropical, Mediterranean, heating-extreme, or low-passive-cooling contexts. Future research should examine climate variation, building type extension, occupational constraint sensitivity, and advanced system configurations such as hydraulic-ventilation hybrids with predictive controls to establish whether findings represent generalizable phenomena or artifacts of the specific case study context.

Keywords:

Holistic Optimization; Building Energy Systems; Building Energy Standards; nZEB; MILP.

1. Introduction

Buildings are fundamental to achieving global decarbonization targets, yet their ecological footprint remains substantial. According to the Intergovernmental Panel on Climate Change (IPCC), global emissions from the building sector reached $12\,\mathrm{GtCO_2}$–eq in 2019, representing $21\,\%$ of global anthropogenic greenhouse gas emissions, with $95\,\%$ attributable to CO_2 [1]. Within the European Union (EU), buildings account for $40\,\%$ of final energy consumption and $36\,\%$ of energy-related emissions, while $75\,\%$ of the building stock remains energy-inefficient [2]. Regulatory intervention through building energy codes has emerged as the primary policy instrument to reduce emissions from both new and existing buildings and has the potential to deliver affordable mitigation solutions [1].

The EU's Energy Performance of Buildings Directive (EPBD) mandates that all new buildings comply with

nearly Zero-Energy Building (nZEB) standards, a requirement in place since 2021 [3]. The recently recast EPBD, effective from 2024, further escalates these requirements further: all new buildings must achieve zero-emission status by 2030, with existing buildings to follow by 2050 [2]. This is defined as zero on-site fossil fuel consumption and very low operational emissions [2]. These stringent energy performance requirements necessitate improved building envelope standards and renewable energy integration to meet compliance standards [4]. Simultaneously, the IPCC emphasizes that immediate action in this decade is critical and that buildings must be adapted to future climate scenarios while ensuring occupant health and well-being, recognizing that anticipated heatwaves will inevitably increase cooling demands [1].

The regulatory trajectory is thus clear: increasingly stringent building envelope insulation standards are mandated to reduce heating-driven energy consumption and operational emissions. Nonetheless, recent empirical evidence has revealed an unintended consequence of the policy framework in question: An increase in cooling loads and overheating due to higher insulation and air tightness of the building envelope, especially in buildings with high internal gains, where heat accumulates. This finding challenges the policy framework's environmental efficacy. This paper investigates this tension through a holistic, ecological and economic optimization approach applied to non-residential buildings.

2. State of the Art

This section addresses four interconnected phenomena established in the literature. Section 2.1 outlines how high-performance building envelopes increase cooling loads under projected climate scenarios. Section 2.2 summarizes thermodynamic capacity limits of surface-based hydraulic heat transfer systems. Section 2.3 highlights the substantial life cycle impact of HVAC distribution systems. Section 2.4 reviews holistic optimization approaches for building energy systems. Finally, Section 2.5 formalizes the specific research gap addressed in this work.

2.1. The Overheating Paradox

Contemporary building regulations mandating enhanced thermal insulation to reduce winter heating demand have produced a counterintuitive outcome. Monitoring of the United Kingdom (UK) housing stock reveals that buildings with the highest energy efficiency ratings (UK Energy performance certificates (EPC) A–C) exhibit overheating in approximately $15\,\%$ of living rooms compared to $10\,\%$ in less-efficient buildings, representing a $50\,\%$ increase in overheating prevalence despite superior thermal performance [5]. Similar patterns are observed in nZEB implementations across Southern European countries, where high-performance buildings in Romania, Italy, Spain, and Belgium frequently experience overheating [6], and in office buildings with high envelope performance, where limited free-running autonomy necessitates active cooling and mechanical ventilation during occupied hours [7].

Across monitored buildings and simulation studies, the quantitative magnitude of this phenomenon is substantial. A Passivhaus dwelling in London is projected to experience cooling loads up to 14 times higher under 2080s conditions compared to 2011 baselines [8]. Climate-forward simulations for Southern Europe indicate large relative increases in residential cooling demand and reduced effectiveness of night ventilation, from $9.3\,\%$ to $5.0\,\%$ in Milan and from $7.6\,\%$ to $3.9\,\%$ in Rome between 2018 and 2060 [9], while residential cooling energy is projected to increase between $32\,\%$ and $101\,\%$ for temperature rises of $1\,^{\circ}\mathrm{C}$ to $2\,^{\circ}\mathrm{C}$ [10]. Mediterranean regions face pronounced increases in heat-wave frequency over 40-year horizons, and field evidence from heat-wave scenarios (up to $43\,^{\circ}\mathrm{C}$ outdoor maximum) demonstrates that even well-insulated buildings require mechanical cooling activation [11]. Although improved envelopes extend passive comfort duration by factors of 2–5 [11], occupants tend to activate air conditioning at comparable temperature thresholds, and refurbishment to nZEB standards can increase thermal discomfort hours by up to $92\,\%$ of the cooling season even in temperate climates [12]. Together, these findings indicate that stringent envelope insulation standards, while reducing heating demand, systematically increase summer cooling requirements and overheating risk in future climates, making mechanical cooling essential to maintain comfort.

2.2. Hydraulic Heat Transfer Systems

The limits of passive cooling imply that mechanical systems will be essential for maintaining thermal comfort in future climates, particularly in heavily insulated non-residential buildings with significant internal gains [9]. Recent investigations show that peak cooling demands, rather than annual loads, increasingly drive required cooling system capacity under projected climate conditions [13].

Surface-based hydraulic heat transfer systems, such as Under Floor Heating (UFH) and Concrete Core Activation (CCA), are widely adopted in nZEB designs. European design guidance acknowledges that these systems can provide part of the cooling energy, but their cooling capacity limits require mechanical ventilation support in balanced or cooling-dominated climates [6]. CCA typically provides approximately $60\,\mathrm{W/m^2}$ cooling and $40\,\mathrm{W/m^2}$ heating at near-room temperatures, so supplementary ventilation and air conditioning are required during peak loads [14]. Real-world operating conditions may modestly increase hydraulic cooling capacity by around $12\,\%$ compared to standardized tests [15], but the systems remain thermally inert and constrained by

maximum and minimum surface temperatures [16]. Consequently, hydraulic systems alone cannot reliably satisfy future peak cooling demands in highly insulated non-residential buildings.

2.3. HVAC Distribution Systems

The capacity constraints of hydraulic heat transfer systems have profound consequences for mechanical ventilation system design in nZEBs. Where hydraulic systems cannot provide sufficient peak cooling, supplementary mechanical ventilation and air conditioning are required to maintain comfort, driving an upsizing cascade throughout the HVAC system and its distribution networks. Despite its design relevance, the life cycle impact of this cascade remains insufficiently quantified in the literature.

Recent life cycle assessment studies demonstrate that HVAC distribution infrastructure contributes a non-negligible share of total embodied emissions over typical building life cycles [17]. As envelope insulation levels and associated air tightness increase, the enlarged mechanical ventilation systems required to compensate for hydraulic capacity limits further amplify this embodied footprint [17]. Existing LCA studies, however, generally compare alternative HVAC configurations for fixed heating and cooling loads and therefore do not capture how distribution system sizing co-varies with envelope performance.

Complementary work on surface-based heating systems indicates slightly lower embodied carbon for floor heating compared to radiators in heating-dominated scenarios [18]. Yet the behavior of such systems under cooling-load constraints remains largely unexplored, and studies that explicitly recognize the importance of HVAC embodied emissions for overall building life cycle impacts [13] do not resolve how distribution and air-handling components should be dimensioned when peak cooling loads dominate. Modern high-performance office buildings exemplify this issue: they employ large-capacity Air Handling Unit (AHU)s that provide both ventilation and thermal load support [7], with sizing influenced by retrofit-driven ventilation requirements and changing heating–cooling balances under climate change [19, 20]. Current European standards mandate energy recovery systems in AHUs, reflecting the architectural shift toward thermally optimized envelopes [21], but regulatory focus remains predominantly on operational energy efficiency.

2.4. Holistic Life Cycle Optimization of Building Energy Systems

The literature reviewed above reveals a critical methodological gap in current nZEB design frameworks: no prior study holistically evaluates building life cycle impacts arising from increased mechanical cooling infrastructure necessitated by high insulation standards. In a recent publication, Höpp et al. [22] showed that previous holistic optimization approaches often rely on simplified system-level emission factors instead of granular component-level quantification or neglect HVAC distribution systems entirely, approximating their impact via percentage surcharges [22].

Addressing these deficiencies, Höpp et al. [22] developed an automated, holistic optimization methodology for non-residential buildings that computes life cycle emissions and costs over construction and a 40-year operational horizon. The model explicitly accounts for embodied and operational impacts of envelope components distribution infrastructure, and energy hub components, and quantifies their interdependence with building thermal dynamics [22]. The methodology performs automated physical dimensioning of hydraulic and air distribution systems based on building topology and simulated thermal demands, using quantity take-offs for embodied emissions and capital costs instead of generic surcharges. An exemplary office building case study indicated that while higher building energy standards can minimize life cycle costs compared to older standards, emission optima span multiple standards due to cooling demand and embodied-emission trade-offs at high insulation levels [22]. However, the hydraulic heat transfer systems in that study were not consistently co-designed with the upsized AHUs and air distribution systems, leading to differing thermal comfort levels across variants and limiting comparability, while the analysis remained closely tied to German code-specific standards.

2.5. Research Gap

Existing work establishes three linked phenomena: (1) stringent envelope insulation standards driven by climate and policy targets increase summer cooling demands in future climates, (2) surface-based hydraulic heating and cooling systems have capacity limits that necessitate mechanical cooling, ventilation, and air conditioning support, and (3) HVAC systems account for a non-negligible share of building life cycle emissions. Nevertheless, the combined effect of these mechanisms has not been quantified. In particular, no peer-reviewed study evaluates how HVAC life cycle emissions and costs scale when component sizing is simultaneously driven by envelope insulation levels and hydraulic heat transfer system capacity constraints under future climate scenarios for non-residential buildings with substantial internal gains.

This paper addresses this gap through holistic life cycle optimization of building energy system design. It examines distinct strategies for providing heating and cooling via hydraulic heat transfer systems and AHUs across a range of building energy standards. By employing the holistic optimization methodology developed by Höpp et al. [22], the work quantifies the previously unexamined trade-off between building energy standards, HVAC system scaling, and life cycle emissions and costs in non-residential buildings.

3. Methodology

This chapter outlines the methodological approach to examine the identified research gaps at the intersection of building envelope performance, hydraulic heat transfer system constraints, and life cycle impacts of HVAC systems. Section 3.1 summarizes the holistic two-stage optimization methodology adopted in this work, which quantifies trade-offs between building energy standards, HVAC system scaling, and life cycle emissions and costs in non-residential buildings under future climate scenarios. Sections 3.2 and 3.3 describe the examined building energy standards, thermal envelope properties, and surface-based heat transfer system configurations, while Sections 3.4 and 3.5 outline the thermal comfort assurance strategy and key boundary conditions.

3.1. Holistic Optimization Approach for Building Energy Systems

The employed methodology follows the holistic optimization approach developed by Höpp et al. [22] for non-residential building energy systems. It uses a two-stage nested optimization to quantify life cycle impacts across construction and a 40-year operational period, with a Pareto formulation balancing life cycle emissions and costs.

The optimization consists of an upper and a lower stage. In Höpp et al. [22], the upper stage employs a black-box algorithm to explore building design variants and Pareto weights between the cost-optimal (0) and emission-optimal (1) extremes [22]. Building design variants combine building energy standard, hydraulic heat transfer system selection, maximum hydraulic supply and return temperatures, and window-to-wall ratio modifications.

In contrast to Höpp et al. [22], this paper replaces the upper-stage black-box search with a full factorial analysis. This modification enables systematic and independent evaluation of the life cycle impacts of building energy standards and hydraulic heat transfer systems, which are treated as design parameters in this work.

For each building design variant and Pareto weight, the lower optimization stage executes a four-step workflow. First, PLUGINTEASER, a plugin of the Python framework *bim2sim* [23], generates and runs Building Energy Performance Simulation (BEPS) models based on the building's Building Information Modeling (BIM) model. These Reduced Order Model (ROM)s are formulated in Modelica using the open-source library AIXLIB [24]. Second, hydraulic and air distribution systems, including the examined heat transfer systems, are created and dimensioned from the BIM-derived geometry and simulated thermal and ventilation demands. Third, embodied emissions and capital costs of the envelope (insulation, windows) and the designed distribution and heat transfer systems are evaluated using material quantity lists. Fourth, a Mixed-Integer Linear Program (MILP)-based design and operational optimization of the building's energy hub is carried out over the 40-year horizon to simultaneously minimize life cycle emissions and costs, considering heating and cooling technologies such as heat pumps, compression chillers, Photovoltaic (PV), and storage systems [22].

3.2. Building Energy Standards Definition

The building energy standards examined in this work are derived from templates in the Python framework TEASER [25], which defines standards based on the thermal properties of exterior wall assemblies consistent with German funding schemes of Kreditanstalt für Wiederaufbau (KfW) and the German Buildings Energy Act (GEG). To increase comparability with international standards, six building energy standards are defined by the exterior wall U-value, ranging from $U_{\text{Wall}} = 0.10\,\mathrm{W/(m^2K)}$ to $U_{\text{Wall}} = 0.35\,\mathrm{W/(m^2K)}$, by adjusting the insulation thickness.

Wall assemblies for exterior walls, ground floor slabs, and roofs are taken from the TEASER templates and remain constant across standards, differing only in the thickness of extruded polystyrene (XPS 30) insulation, a common building insulation material [26]. U-values of ground slabs and roofs are obtained by interpolating between KfW reference values as a function of U_{Wall}, and the resulting insulation thicknesses are derived from these interpolated U-values. Interior component U-values (interior walls, floor slabs, ceiling assemblies) remain constant across standards and follow the KfW–TEASER templates. Window thermal transmittance increases with decreasing insulation level to reflect regulatory consistency, while base infiltration rates decrease with higher building energy standards to represent tighter envelopes. The resulting insulation thicknesses, window configurations, and base infiltration rates per standard are summarized in Table 1.

3.3. Surface-Based Heat Transfer Systems and Air Handling Unit Configuration

In addition to the six building energy standards, three surface-based hydraulic heat transfer system configurations are examined, each combined with an AHU that provides complementary peak-load capacity. Two UFH variants are installed within the floor assembly with installation depths of $25\,\mathrm{mm}$ (UFH_{25}) and $55\,\mathrm{mm}$ (UFH_{55}). Owing to condensation risk in cooling mode, UFH systems deliver exclusively base-load heating, while the AHU supplies peak-load heating and both base- and peak-load cooling, including dehumidification and humidification via energy-efficient heat recovery with a dynamic bypass controller.

A single CCA variant is implemented in ceiling assemblies with an installation depth of $100\,\mathrm{mm}$ (CCA_{100}). It provides both heating and cooling base-load capacity through two independent hydraulic circuits, with the AHU again supplying supplementary peak-load heating and cooling and air conditioning services. All surface-based

Table 1. *Building Energy Standards: Insulation Thickness, U-Values, Base Infiltration, and Window Properties*

Building Energy Standard	Outer Wall		Roof		Ground Floor		Base Infiltr.	Window
	Insul. Thick. in m	U-Value in W/m²K	Insul. Thick. in m	U-Value in W/m²K	Insul. Thick. in m	U-Value in W/m²K	in h^{-1}	g-Value
$U_{0.10}$	0.2984	0.10	0.4722	0.0685	0.3383	0.1157	0.04	0.50
$U_{0.15}$	0.1618	0.15	0.2925	0.1056	0.2082	0.1828	0.07	0.50
$U_{0.20}$	0.0934	0.20	0.1920	0.1516	0.1227	0.2954	0.10	0.65
$U_{0.25}$	0.0524	0.25	0.1307	0.2065	0.0956	0.3670	0.14	0.65
$U_{0.30}$	0.0251	0.30	0.106	0.2417	0.0833	0.4125	0.20	0.67
$U_{0.35}$	0.0056	0.35	0.0876	0.277	0.0735	0.4579	0.30	0.67

systems exhibit inert thermal behavior and respond slowly to peak loads. To represent this in the ROMs, Höpp et al. [22] proposed a simplified PT1-element approach, with parameters derived from detailed simulations using the open-source Modelica library BESMOD [22, 27].

3.4. Thermal Comfort Assurance Across

To ensure comparable thermal comfort and occupant conditions across all combinations of building energy standards and surface-based heat transfer systems, the AHU provides dynamic support to the hydraulic systems during peak loads. The control strategy adjusts two key variables: the air volume flow rate per thermal zone and the central air supply temperature.

Maximum feasible air volume flow is increased according to the thermal inertia of each heat transfer system, and the air distribution network and AHU capacity are dimensioned accordingly. Controller integration time constants governing AHU operation are likewise tuned to the inertia characteristics of the respective system, ensuring sufficiently responsive yet stable thermal control.

3.5. Boundary Conditions

The analysis incorporates several boundary conditions to establish a realistic operational framework. Dynamic solar shading is employed to limit solar gains: automated blinds close when solar irradiance reaches $I = 200\,\mathrm{W/m^2}$ and reduce transmitted radiation by $70\,\%$. Internal gains are assigned per zone type according to DIN V 18599-10 [28].

Infiltration comprises four components: base infiltration per building energy standard (cf. Section 3.2), activity-dependent infiltration in occupied zones, temperature-dependent infiltration during summer, and adaptive passive ventilation up to 3 air changes per hour when overheating is detected, with the rate scaled to the overheating magnitude to limit reliance on mechanical cooling.

The energy hub designed in the MILP-based optimization consists exclusively of electrified technologies. Heating is provided by air-, probe-, or collector-sourced heat pumps and electric heaters, while cooling is supplied by compression chillers and reversible heat pumps. Thermal energy storage for heating and cooling, on-site electricity generation via PV, battery storage, and grid electricity supply are included. The AHU offers air-conditioning functions, including dehumidification and humidification. Meteorological data are taken from German Test Reference Year (TRY) datasets of German Meteorological Service (DWD) for current conditions and 2045 climate projections, representing the DWD's base climate scenarios without extreme events [29].

Dynamic hourly electricity prices and associated emission factors are derived from 2024 German market data [30]. Cost parameters for energy-hub technologies are obtained from BAUKOSTENINFORMATIONSZENTRUM DEUTSCHER ARCHITEKTENKAMMERN (BKI) [31] and the TECHNIKKATALOG WÄRMEWENDE [32], emission factors from the ÖKOBAUDAT database [33], and technical parameters from the TECHNIKKATALOG WÄRMEWENDE [32]. Heat pump and compression chiller performance are represented using characteristic maps from WAMAK and CARRIER, respectively [34, 35]. For further details on boundary conditions and parameter selections, please refer to Höpp et al. [22].

4. Results

The subsequent sections present the results obtained with the described methodology. Section 4.1 first introduces the case study building to which the holistic optimization is applied. The analysis then examines life cycle emissions and costs across distinct building energy standards and surface-based heat transfer system configurations using a full factorial design. Pareto-optimal solutions are reported by heat transfer system in Section 4.2 and by building energy standard in Section 4.3, followed by component-level analyses in Sections 4.4 and 4.5 that explain how heat transfer system and envelope choices drive HVAC scaling and life cycle

impacts.

4.1. Application of the methodology to a case study building

The methodology is applied to a typical non-residential office building located in Aachen, Germany. The building is modeled in BIM format according to the Industry Foundation Classes (IFC)4 standard, based on a reference architectural model from the Karlsruhe Institute of Technology [36]. It comprises three stories above a basement with a net conditioned area of $1939\,\mathrm{m}^2$. The envelope includes $901.4\,\mathrm{m}^2$ of exterior walls and $309.5\,\mathrm{m}^2$ of window area, with the long facades oriented north–south and the short facades east–west and only minimal glazing on the latter.

4.2. Life cycle impacts differentiated by heat transfer system

Section 4.2 presents the Pareto cloud and the derived Pareto fronts per heat transfer system. The analysis reveals substantial differences in life cycle performance across the three heat transfer system variants examined with pronounced separation of the respective Pareto fronts. This suggests that system selection is a critical determinant of life cycle performance independent of building energy standard variation.

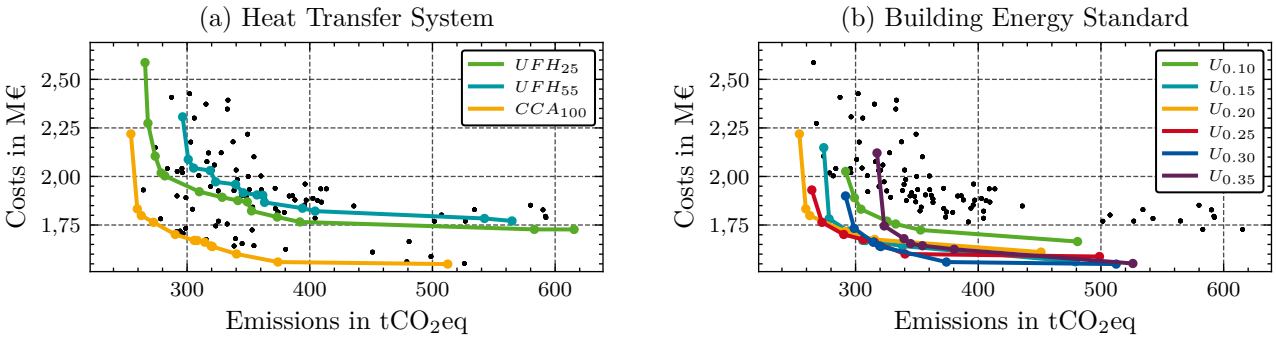

Figure 1. *Pareto cloud of all solutions of building design variants and Pareto weights with their respective life cycle emissions and costs as well as optimal Pareto fronts (a) per hydraulic heat transfer system and (b) per building energy standard.*

A detailed analysis shows that the CCA_{100} system demonstrates superior performance across both objectives. The cost-optimal CCA_{100} solution at $1.55\,\mathrm{M€}$ reduces life cycle costs by $10.4\,\%$ compared to UFH_{25} ($1.73\,\mathrm{M€}$) and $12.4\,\%$ compared to UFH_{55} ($1.77\,\mathrm{M€}$). The emission-optimal CCA_{100} solution at $254\,\mathrm{tCO_2}$–eq lowers emissions by $4.5\,\%$ relative to UFH_{25} ($266\,\mathrm{tCO_2}$–eq) and $14.2\,\%$ relative to UFH_{55} ($296\,\mathrm{tCO_2}$–eq).

4.3. Life cycle impacts differentiated by building energy standard

Section 4.2 presents the Pareto cloud and Pareto fronts for each building energy standard. In line with the previous analysis, the corresponding optimal solutions employ the CCA_{100} heat transfer system. Unlike the pronounced differentiation between heat transfer systems, no single building energy standard dominates across all Pareto weights.

The $\mathrm{U}_{0.20}$ standard yields emissions-optimal solutions at $254\,\mathrm{tCO_2}$–eq, corresponding to $13.0\,\%$ lower emissions than $\mathrm{U}_{0.10}$ ($292\,\mathrm{tCO_2}$–eq) and $19.9\,\%$ lower emissions than $\mathrm{U}_{0.35}$ ($317\,\mathrm{tCO_2}$–eq). Cost-optimal solutions occur at $\mathrm{U}_{0.30}$ with $1.55\,\mathrm{M€}$, representing a $6.6\,\%$ cost reduction relative to $\mathrm{U}_{0.10}$ ($1.66\,\mathrm{M€}$). The highest insulation level $\mathrm{U}_{0.10}$ is least favorable at the cost-optimal end of the Pareto front and near-worst at the emission-optimal end, whereas $\mathrm{U}_{0.15}$ performs substantially better. For intermediate Pareto weights, life cycle emissions and costs with $\mathrm{U}_{0.15}$ deviate by only about $1\,\%$ to $2\,\%$ from the best solutions at $\mathrm{U}_{0.20}$ and $\mathrm{U}_{0.25}$. A more detailed component-level interpretation is provided in Section 4.5.

4.4. Component-Level Decomposition by Heat Transfer System

Figure 2 decomposes life cycle emissions and costs by component group across the three examined hydraulic heat transfer systems, all evaluated at constant building energy standard $\mathrm{U}_{0.25}$. Yearly energy demands and peak loads for heating and cooling, as well as maximum and average ventilation flow rates, are presented alongside life cycle impacts.

Building envelope emissions and costs remain constant across heat transfer system variants due to identical insulation specification at $\mathrm{U}_{0.25}$, representing $10\,\%$ to $13\,\%$ of total emissions and $15\,\%$ to $20\,\%$ of total costs. Distribution system embodied impacts exhibit minor variation, constituting approximately $5\,\%$ of total emissions and $15\,\%$ of total costs, though CCA_{100} systems incur elevated costs due to dual hydraulic networks required for independent heating and cooling circuits.

Energy hub embodied emissions and costs vary substantially across heat transfer systems, representing $40\,\%$ to $45\,\%$ of total life cycle impacts. The CCA_{100} system achieves the lowest embodied impacts, while UFH

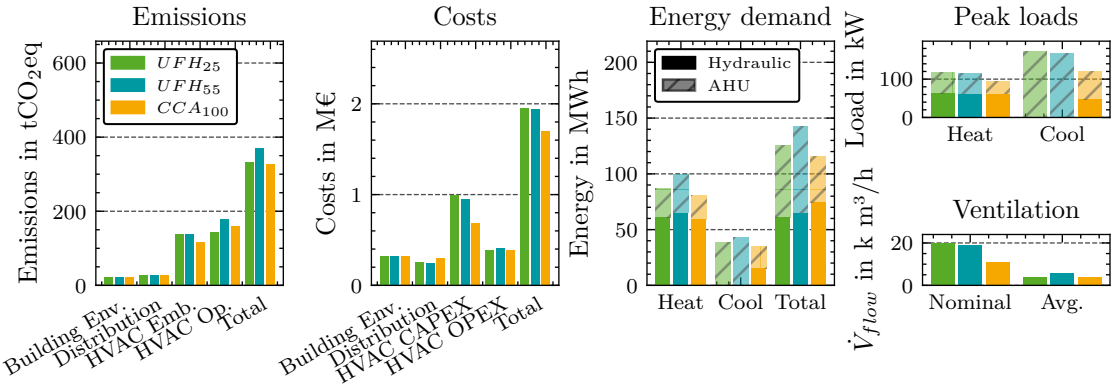

Figure 2. *Distribution of life cycle emissions and costs per component group, yearly energy demands, peak loads, and ventilation demands across heat transfer systems at a constant building energy standard ($U_{0.25}$).*

systems exhibit intermediate values. Energy hub operational emissions and costs demonstrate pronounced differentiation, constituting $40\,\%$ to $45\,\%$ of total emissions but only $15\,\%$ to $20\,\%$ of total costs. The UFH_{25} and CCA_{100} configurations achieve the lowest operational impacts, while UFH_{55} exhibits increased values.

The critical mechanism driving these impacts emerges from heat transfer system-dependent peak load characteristics. Equivalent hydraulic heating peak loads are maintained near $62\,\mathrm{kW}$ across systems. However, AHU peak heating demands differ substantially: CCA_{100} requires the lowest peak loads, while UFH_{25} and UFH_{55} systems require $74.6\,\%$ and $71.5\,\%$ higher loads, respectively. Similarly, peak cooling loads via the AHU diverge dramatically: CCA_{100} provides hydraulic base cooling, requiring the AHU to supply peak cooling capacity only, while UFH systems necessitate the AHU to provision all cooling capacity simultaneously, given the condensation risk that is present during the cooling mode operation of UFH systems.

The higher AHU heating and cooling peak loads with UFH systems compared to CCA_{100} are associated with the required ventilation systems. Maximum air volume flow with CCA_{100} is approximately $10\,900\,\mathrm{m^3/h}$. UFH systems necessitate approximately $100\,\%$ greater maximum volume flow, reflecting the fact that these systems provide no hydraulic cooling. Consequently, the AHU must supply the entire cooling capacity through enlarged air volume flows. Average air volume flow follows parallel behavior: $3866\,\mathrm{m^3/h}$ with CCA_{100}, increasing $9\,\%$ with UFH_{25} and $56\,\%$ with UFH_{55}. The elevated average flows reflect the continuous base-load and peak-load cooling requirement throughout cooling periods.

Larger air volume flows necessitate increased supply air conditioning. Reheating energy following supply air dehumidification constitutes $62\,\%$ of AHU heating demand with CCA_{100}, increasing to $76\,\%$ with UFH_{25} due to enlarged air volume flows during cooling periods. Consequently, total cooling energy demands with UFH systems exceed CCA_{100} by $11\,\%$ (UFH_{25}) to $22\,\%$ (UFH_{55}), despite identical thermal comfort conditions. This mechanism-peak load-driven air volume increases necessitating greater dehumidification-cascades through embodied impacts of enlarged AHU and distribution systems, explaining the substantial life cycle cost and emission differences observed across heat transfer systems. Qualitatively identical patterns persist across all building energy standards examined, confirming that heat transfer system selection is a dominant driver of HVAC system scaling and embodied life cycle impacts independent of envelope insulation level.

4.5. Component-Level Decomposition by Building Energy Standard

Figure 3 decomposes life cycle emissions and costs by component groups across the six examined building energy standards at a constant heat transfer system (CCA_{100}), isolating the independent effect of envelope insulation variation. Furthermore, heating and cooling peak loads and yearly demands as well as nominal and average ventilation demands are visualized.

Embodied building envelope emissions and costs increase monotonically with higher insulation levels, rising $399\,\%$ in emissions and $133\,\%$ in costs from $U_{0.35}$ to $U_{0.10}$. Envelope impacts represent $10\,\%$ to $28\,\%$ of total emissions and $12\,\%$ to $26\,\%$ of total costs. Distribution system emissions and costs exhibit minimal variation across standards, increasing only $6\,\%$ in emissions and $2\,\%$ in costs across the full insulation range, reflecting that distribution sizing is driven by peak thermal loads rather than total energy demands. Energy hub embodied emissions and costs also tend to rise slightly with lower building energy standards, with operational impacts decreasing $38.4\,\%$ in emissions and $28.9\,\%$ in costs from $U_{0.35}$ to $U_{0.10}$ due to reduced heating demands.

Peak load constraints present a fundamental limitation on the benefits of increased insulation. Hydraulic heating peak loads decrease approximately $60\,\%$ from $U_{0.35}$ to $U_{0.10}$, following the reduction in heating demand. Hydraulic cooling peak loads exhibit the same behavior, increasing approximately $53.3\,\%$, due to less insulation

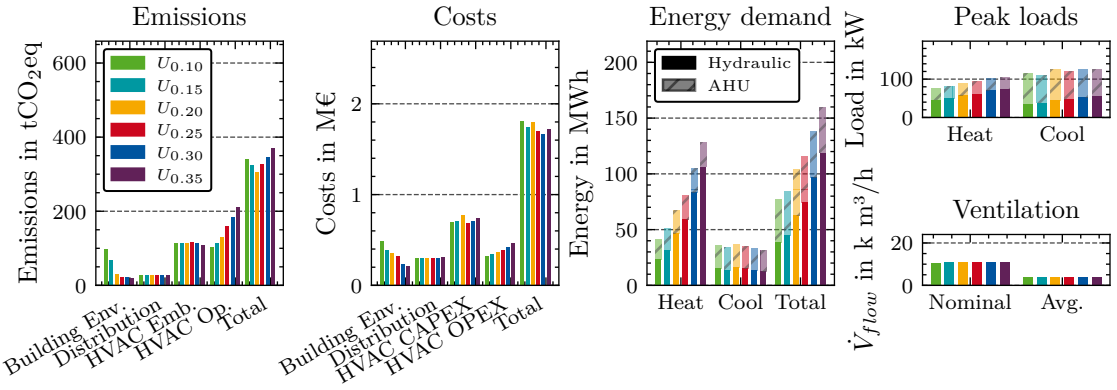

Figure 3. *Distribution of life cycle emissions and costs per component group, yearly energy demands, peak loads, and ventilation demands across building energy standards at constant heat transfer system (CCA_{100}).*

and air tightness as well as lower quality windows, which allow solar radiation to pass through, at hot summer days. Inversely, yearly hydraulic cooling demands increase with higher building energy standards due to higher heat accumulation in cooling hours away from days of extreme weather.

Despite these changes in hydraulic system loads, AHU peak cooling demand remains approximately constant across building energy standards. This constant AHU cooling capacity requirement prevents corresponding reductions in embodied impacts of distribution systems and energy hub components across the insulation range, even as heating energy decreases substantially. While heating demands dominate cooling demands by margins ranging from $16.3\,\%$ excess at $U_{0.10}$ to $306.7\,\%$ excess at $U_{0.35}$, the peak cooling loads exceed peak heating loads, creating a binding constraint on system downsizing. High-performance passive cooling strategies, including infiltration-based overheating relief, significantly reduce mechanical cooling demands, yet peak load requirements during design conditions remain the primary driver of AHU and distribution system sizing.

Maximum and average air volume flow rates increase slightly with lower building energy standards, reflecting that system dimensioning is governed by peak the thermal load provision rather than annual energy demands. Ventilation demands are therefore insensitive to envelope insulation variations when dynamic thermal comfort control is employed. The absence of a universally superior building energy standard reflects the coupling between envelope embodied impacts and operational thermal demands. Higher insulation increases envelope embodied emissions and capital costs while reducing heating-driven operational energy. Simultaneously, higher insulation elevates cooling demands. Peak cooling loads, constrained by dynamic control requirements, maintain constant AHU sizing and prevent significant embodied emission and cost reductions in distribution and energy hub systems. This peak-load-driven sizing mechanism explains why medium insulation standards ($U_{0.20}$ to $U_{0.25}$) achieve optimal life cycle emissions and costs. These standards balance envelope embodied impacts, operational heating reductions, and cooling peak load constraints, producing the minimum life cycle burden across ecological and economic objectives.

5. Discussion

This paper examines how mandated envelope insulation standards can unintentionally increase mechanical cooling infrastructure, challenging the assumption that stricter standards always reduce life cycle emissions in uniform nZEB frameworks. The results reveal competing mechanisms that produce a non-monotonic relationship between building energy standards, peak cooling-driven HVAC sizing, and life cycle performance.

The analysis confirms that peak thermal load constraints, rather than annual energy demand, govern the sizing of the AHU. Across all building energy standards, peak cooling loads exceed peak heating loads, so the required AHU capacity remains nearly constant even as heating energy decreases substantially. This decoupling between annual operational energy and peak-load-driven HVAC sizing prevents proportional reductions in the embodied impacts of distribution systems and energy hub components.

The building envelope amplifies this trade-off. Increasing insulation thickness and window performance substantially raises embodied emissions and costs of opaque elements, while reducing heating energy but increasing cooling loads. At the highest insulation level, additional envelope embodied burdens are no longer offset by operational heating savings, leading to worse life cycle performance than for medium insulation standards.

The Pareto front analysis reflects this mechanism directly. The $U_{0.20}$ standard achieves emission-optimal solutions, representing $13\,\%$ lower emissions compared to $U_{0.10}$ and $19.9\,\%$ lower emissions than $U_{0.35}$. The $U_{0.30}$ standard achieves cost-optimal solutions, representing $6.6\,\%$ cost reduction compared to $U_{0.10}$. Across

intermediate Pareto weights, the $U_{0.20}$ and $U_{0.25}$ standards exhibit optimal solutions, indicating that moderate insulation levels balance envelope embodied impacts, operational heating reductions, and cooling peak load constraints most effectively....

Heat transfer system selection emerges as a dominant determinant of life cycle performance, exceeding the influence of building envelope standards. The CCA_{100} system achieves $29.2\,\%$ life cycle emission reduction compared to alternatives, while building energy standard variation yields only $19.9\,\%$ emission reduction. Cost impacts prove more pronounced: heat transfer system choice produces $37.8\,\%$ cost reductions compared to $6.6\,\%$ reductions from building standard selection. This dominance results directly from peak load-driven system design mechanisms. The CCA_{100} system provides hydraulic base cooling capacity, requiring the AHU to supply only peak cooling load, thereby achieving maximum efficiency, also due to improved efficiency levels resulting from higher cooling temperatures. In contrast, UFH systems provide no hydraulic cooling capacity, necessitating the AHU to supply all cooling loads simultaneously with necessary lower temperature levels than with hydraulic heat transfer systems. This design necessity results in approximately $100\,\%$ larger maximum volume flows with UFH systems compared to CCA_{100}. The ventilation cascade propagates through embodied impacts as enlarged distribution systems and energy hub components become necessary to accommodate these amplified air volume requirements.

Passive measures such as automated solar shading and adaptive infiltration relieve overheating and reduce annual cooling energy but do not remove the peak cooling constraints that drive AHU sizing. Under projected future climates, the effectiveness of night ventilation further declines [9], so embodied impacts of air-side systems remain largely governed by design-day loads rather than by annual cooling energy. Exploring design strategies that explicitly relax peak-load criteria or accept slightly higher thermal discomfort could therefore offer additional life cycle benefits.

Taken together, these results suggest that the monotonic logic underpinning current building energy standards-assuming that more insulation always improves life cycle performance-is not generally valid for temperate office buildings with high internal gains. In such contexts, high insulated envelopes can increase envelope-related embodied impacts without enabling downsizing of HVAC systems and can exacerbate cooling-driven peak loads, undermining the intended environmental benefits [8, 9].

However, it is imperative to acknowledge the limitations that constrain the generalizability of these findings, as these results are specific for a single non-residential office building, located in Aachen, Germany: The passive cooling strategies adopted represent specific design choices with inherent sensitivities. The study does not explore variations in passive cooling system specifications, such as differentiated night and day ventilation strategies compliant with occupational safety constraints on maximum air velocity. These constraints may fundamentally limit passive cooling feasibility in occupied zones, thereby altering the embodied-operational impact balance.

Additionally, the analysis holds constant several design parameters that merit independent investigation: The case study building features long facades oriented north and south. Buildings with different orientations may exhibit altered heating-cooling load and demand balances. Moreover, the size of the building and its type of use may cause shifts in the balance between heating and cooling loads and demands, due to distinct internal heat gains. Furthermore, the sensitivity of life cycle impacts to insulation material selection - particularly low-emission or cost-optimized insulation materials - remains unexplored. AHU operational strategies, including dynamic modulation of circulating air volume flows in response to varying thermal loads, were not examined as optimization levers.

The building's location in Aachen, Germany, represents a temperate climate region where heating demands dominate cooling demands and high-performance passive cooling systems are feasible. This geographic and climatic constraint significantly limits generalization. Results cannot be reliably extended to tropical, Mediterranean, heating-extreme, or low-passive-cooling contexts, where the heating-cooling load and demand balance and resulting life cycle impacts would differ substantially.

These limitations bound the scope of recommendations to buildings sharing the geometric, climatic, and operational characteristics of the examined case study. Broader applicability requires systematic extension across climate zones, building types, and design configurations to establish whether the non-monotonic optimization relationship and heat transfer system dominance documented herein represent generalizable phenomena or artifacts of the specific temperate, office-building context.

6. Conclusion

This paper addresses a critical gap at the intersection of three well-established phenomena: First, stringent building energy standards increase summer cooling demands in future climates. Second, surface-based hydraulic heat transfer systems have capacity limits necessitating mechanical ventilation support. Third, HVAC systems account for non-negligible life cycle impacts. No prior peer-reviewed study quantified how the life cycle emissions and costs of HVAC systems scale when component sizing is driven by building insulation, combined

with capacity constraints of hydraulic heat transfer systems in future climate scenarios for non-residential buildings.

This work employs the holistic optimization methodology developed by Höpp et al. [22], which holistically, optimizes life cycle emissions and life cycle costs across construction and a 40-year operational period through BEPS, physically-dimensioned distribution system design, Life Cycle Assessment (LCA) & Life Cycle Cost (LCC), and MILP-based energy hub optimization. The methodology enables component-level quantification of life cycle emissions and costs rather than relying on simplified percentage surcharges, rendering the interdependence between the building envelope and embodied and operational impacts of the HVAC system, consisting of the energy hub, distribution and heat transfer systems.

The examination of six distinct building energy standards and three distinct hydraulic heat transfer system configurations across a non-residential office building in Aachen, Germany, under 2045 climate projections reveals two principal findings. First, the CCA_{100} system demonstrates superior life cycle performance compared to UFH systems through its capacity to provide hydraulic base cooling, thereby minimizing AHU sizing and associated distribution system embodied impacts. Second, a non-monotonic relationship exists between building envelope insulation and life cycle performance. Medium insulation standards at $U_{0.20}$ to $U_{0.25}$ achieve optimal life cycle emissions and costs, while the highest insulation standard at $U_{0.10}$ yields $13\,\%$ higher emissions than $U_{0.20}$. This paradox results from competing mechanisms: higher insulation increases envelope embodied impacts substantially, while peak cooling load constraints prevent corresponding reductions in mechanical system embodied impacts, even as operational heating demands decline significantly.

These findings indicate that building energy standards emphasizing uniform envelope insulation levels may be suboptimal for the examined building type, even in temperate climates employing high-performance passive cooling. Rather than prescriptive U-value mandates, climate-specific standards enabling envelope-system trade-offs are therefore recommended. Heat transfer system selection should receive policy priority equal to envelope insulation standards in non-residential office buildings. Future nZEB shall be optimized holistically - with envelope, hydraulic, and ventilation systems co-sized for simultaneous energy efficiency and life cycle emission and cost minimization, adapting designs to location-specific constraints and climate scenarios.

Several important limitations bound these conclusions. The analysis examines a single non-residential office building in Aachen, Germany, within a temperate climate with high-performance passive cooling systems. Therefore, the results are not generalizable to tropical, Mediterranean, heating-extreme, or low-passive-cooling contexts. Building type variation, building size, orientation, and insulation material sensitivity remain unexplored. Future research should examine climate variation, building type extension, occupational constraint sensitivity, and advanced system configurations such as hydraulic-ventilation hybrids with predictive controls.

Acknowledgments

We gratefully acknowledge the financial support of the German *Federal Ministry for Economic Affairs and Energy* (BMWE) - Grant number: 03EN3026C.

References

[1] Cabeza, L. F., Q. Bai, P. Bertoldi, J.M. Kihila, A.F.P. Lucena, É. Mata, S. Mirasgedis, A. Novikova, Y. Saheb, Buildings. In IPCC, in: Climate Change 2022: Mitigation of Climate Change. Contribution of Working Group III to the Sixth Assessment Report of the Intergovernmental Panel on Climate Change, volume IPCC Sixth Assessment Report, Working Group III: Mitigation of Climate Change of *IPCC Sixth Assessment Report*, 1 edition, Cambridge University Press, 2022, pp. 953–1048. URL: https://www.cambridge.org/core/product/identifier/9781009157926%23c9/type/book_part. DOI: 10.1017/9781009157926.011.

[2] Directive (EU) 2024/1275 of the European Parliament and of the Council of 24 April 2024 on the Energy Performance of Buildings (Recast) (Text with EEA Relevance), 2024. URL: http://data.europa.eu/eli/dir/2024/1275/oj.

[3] Directive 2010/31/EU of the European Parliament and of the Council of 19 May 2010 on the Energy Performance of Buildings (Recast), 2021. URL: http://data.europa.eu/eli/dir/2010/31/2021-01-01.

[4] Buildings Performance Institute Europe (BPIE), Nearly Zero: A Review of EU Member State Implementation of New Build Requirements, Buildings Performance Institute Europe (BPIE), 2021. URL: https://www.bpie.eu/publication/nearly-zero-a-review-of-eu-member-state-implementation-of-new-build-, last accessed: 2026-03-19.

[5] Climate Change Committee, Risks to Health, Wellbeing and Productivity from Overheating in Buildings, 2022. URL: https://www.theccc.org.uk/wp-content/uploads/2022/07/Risks-to-health-wellbeing-and-productivity-from-overheating-in-buildings.pdf, last ac-

cessed: 2026-03-19.

[6] S. Attia, P. Eleftheriou, F. Xeni, R. Morlot, C. Ménézo, V. Kostopoulos, M. Betsi, I. Kalaitzoglou, L. Pagliano, M. Cellura, M. Almeida, M. Ferreira, T. Baracu, V. Badescu, R. Crutescu, J. M. Hidalgo-Betanzos, Overview and future challenges of nearly zero energy buildings (nZEB) design in Southern Europe, Energy and Buildings 155 (2017) 439–458. URL: https://linkinghub.elsevier.com/retrieve/pii/S0378778817331195. DOI: 10.1016/j.enbuild.2017.09.043.

[7] A. Sengupta, J. Deleu, B. Lucidarme, H. Breesch, M. Steeman, Assessing thermal resilience to overheating in an office building, in: Conference on Indoor Environmental Quality Performance Approaches 2020, Pt. 1, American Society of Heating, Refrigerating and Air-Conditioning Engineers (ASHRAE), Athens, Greece, 2021, pp. 33–40. URL: http://hdl.handle.net/1854/LU-01GZP0Z0BEH5AX8A9ZCKSETXNC.

[8] M. Alrasheed, M. Mourshed, Domestic overheating risks and mitigation strategies: The state-of-the-art and directions for future research, Indoor and Built Environment 32 (2023) 1057–1077. URL: https://journals.sagepub.com/doi/10.1177/1420326X231153856. DOI: 10.1177/1420326X231153856.

[9] D. D'Agostino, D. Parker, I. Epifani, D. Crawley, L. Lawrie, How will future climate impact the design and performance of nearly zero energy buildings (NZEBs)?, Energy 240 (2022) 122479. URL: https://www.sciencedirect.com/science/article/pii/S0360544221027286. DOI: 10.1016/j.energy.2021.122479.

[10] F. Mancini, G. Lo Basso, How Climate Change Affects the Building Energy Consumptions Due to Cooling, Heating, and Electricity Demands of Italian Residential Sector, Energies 13 (2020) 410. URL: https://www.mdpi.com/1996-1073/13/2/410. DOI: 10.3390/en13020410.

[11] C. M. Calama-González, R. Escandón, A. Alonso, R. Suárez, L. León-Rodríguez, A. Sánchez-Ostiz Gutiérrez, A. Arriazu-Ramos, A. Monge-Barrio, Thermal insulation impact on overheating vulnerability reduction in Mediterranean dwellings, Heliyon 9 (2023) e16102. URL: https://linkinghub.elsevier.com/retrieve/pii/S2405844023033091. DOI: 10.1016/j.heliyon.2023.e16102.

[12] M. P. Tootkaboni, I. Ballarini, V. Corrado, Analysing the future energy performance of residential buildings in the most populated Italian climatic zone: A study of climate change impacts, Energy Reports 7 (2021) 8548–8560. URL: https://www.sciencedirect.com/science/article/pii/S2352484721002274. DOI: 10.1016/j.egyr.2021.04.012.

[13] R. Rahif, A. Norouziasas, E. Elnagar, S. Doutreloup, S. M. Pourkiaei, D. Amaripadath, A.-C. Romain, X. Fettweis, S. Attia, Impact of climate change on nearly zero-energy dwelling in temperate climate: Time-integrated discomfort, HVAC energy performance, and GHG emissions, Building and Environment 223 (2022) 109397. URL: https://www.sciencedirect.com/science/article/pii/S0360132322006308. DOI: 10.1016/j.buildenv.2022.109397.

[14] F. Mauersberger, D. Cibis, Energy Efficiency In Commercial Buildings With Concrete Core Activation, in: Proceedings from the International High Performance Buildings Conference 2012, Purdue, USA, 2012. URL: http://docs.lib.purdue.edu/ihpbc/64.

[15] T. Burger, Factors Which Increase the Capacity of Radiant Ceilings: Difference between EN 14240 and Reality, Barcol-Air Group AG, 2024. URL: https://www.barcolair.com/media/filer_public/14/a3/14a36f5f-422b-42cf-8ef4-a73326bf8770/factors_which_increase_the_capacity.pdf, last accessed: 2026-03-19.

[16] P. van den Engel, R. Bokel, L. de Ruijsscher, Concrete core activation, Kennisbank Bouwfysica (2009) I–431. URL: https://klimapedia.nl/wp-content/uploads/2013/05/I-432-Concrete-core-activation-WP+GA_v0.0.pdf, last accessed: 2026-03-19.

[17] R. H. Crawford, P. Gobinath, K. Thomson, An approach for comparing the embodied greenhouse gas emissions of HVAC systems for large volume buildings, in: Harmony in Architectural Science and Design: Sustaining the Future. Proceedings of the 57th International Conference of the Architectural Science Association 2024, Australia and New Zealand Architectural Science Association, Gold Coast, Australia, 2024.

[18] L. Z. Gergely, E. Barna, M. Horváth, Z. Szalay, Assessing embodied and operational carbon of residential HVAC systems: Baselines for life-cycle sustainability, Building and Environment 269 (2025) 112442. URL: https://www.sciencedirect.com/science/article/pii/S0360132324012836. DOI: 10.1016/j.buildenv.2024.112442.

[19] D. Vakalis, E. Diaz Lozano Patino, T. Opher, M. F. Touchie, K. Burrows, H. L. MacLean, J. A. Siegel, Quantifying thermal comfort and carbon savings from energy-retrofits in social housing, Energy and Buildings 241 (2021) 110950. URL: https://www.sciencedirect.com/science/article/pii/S0378778821002346. DOI: 10.1016/j.enbuild.2021.110950.

[20] C. Fieberg, D. Demmelhuber, Impact of Climate Change on the Design of Air Handling Units, in: The

14th REHVA HVAC World Congress, Rotterdam, Netherlands, 2022. URL: https://proceedings.open.tudelft.nl/clima2022/article/view/360. DOI: 10.34641/clima.2022.360.

[21] Eurovent, Eurovent Guidebook: Air Handling Units, Eurovent, 2021. URL: https://www.eurovent.eu/wp-content/uploads/2021-eurovent-ahu-guidebook-second-edition-en-web.pdf, last accessed: 2026-03-19.

[22] J. Höpp, D. Jansen, N. Fuchs, D. Müller, Holistic, ecological, and economic optimization of non-residential buildings based on OpenBIM, Preprint submitted to Energy and Buildings (2026). URL: http://ssrn.com/abstract=6110379. DOI: 10.2139/ssrn.6110379.

[23] D. Jansen, V. Richter, L. Maier, J. Frisch, C. van Treeck, D. Müller, Open-source framework for automated generation of building energy performance simulation models and beyond from BIM Data, Automation in Construction 179 (2025) 106427. DOI: https://doi.org/10.1016/j.autcon.2025.106427.

[24] L. Maier, D. Jansen, F. Wüllhorst, M. Kremer, A. Kümpel, T. Blacha, D. Müller, Aixlib: an open-source modelica library for compound building energy systems from component to district level with automated quality management, Journal of Building Performance Simulation 17 (2023) 196–219. DOI: https://doi.org/10.1080/19401493.2023.2250521.

[25] P. Remmen, M. Lauster, M. Mans, M. Fuchs, T. Osterhage, D. Müller, TEASER: An open tool for urban energy modelling of building stocks, Journal of Building Performance Simulation 11 (2018) 84–98. DOI: https://doi.org/10.1080/19401493.2017.1283539.

[26] European Commission. Joint Research Centre., Competitive Landscape of the EU's Insulation Materials Industry for Energy-Efficient Buildings: Revised Edition., Publications Office, 2018. URL: https://data.europa.eu/doi/10.2760/750646.

[27] F. Wüllhorst, L. Maier, D. Jansen, L. Kühn, D. Hering, D. Müller, BESMod - A Modelica Library providing Building Energy System Modules, in: Proceedings of the American Modelica Conference 2022, Dallas, USA, 2022, pp. 9–18. DOI: https://doi.org/10.3384/ecp211869.

[28] Standard DIN V 18599-10:2018-09: Energy efficiency of buildings - Calculation of the net, final and primary energy demand for heating, cooling, ventilation, domestic hot water and lighting - Part 10: Boundary conditions of use, climatic data, German Institute for Standardization (DIN), Berlin, Germany, 2018. DOI: https://doi.org/10.31030/2874436.

[29] G. M. S. (DWD), Handbuch: Ortsgenaue Testreferenzjahre von Deutschland für mittlere, extreme und zukünftige Witterungsverhältnisse, Offenbach, Germany, 2017. URL: https://www.bbsr.bund.de/BBSR/DE/forschung/programme/zb/Auftragsforschung/5EnergieKlimaBauen/2013/testreferenzjahre/try-handbuch.pdf?__blob=publicationFile&v=3, last accessed: 2026-03-19.

[30] Agora Energiewende, Agorameter, Berlin, Germany, 2025. Version 4.1.1, URL: https://www.agora-energiewende.de/daten-tools/agorameter, last accessed: 2025-10-11.

[31] Baukosteninformationszentrum (BKI), BKI Baukosten 2024 Neubau Teil 2: Statistische Kostenkennwerte für Bauelemente, BKI Kostenplanung, Baukosteninformationszentrum Deutscher Architektenkammern GmbH, Stuttgart, Germany, 2024. ISBN: 978-3-481-04743-6.

[32] N. Langreder, F. Lettow, M. Sahnoun, S. Kreidelmeyer, S. Lengning, Technikkatalog Wärmeplanung, Institut für Energie- und Umweltforschung Heidelberg (ifeu), Öko-Institut e.V., IER Stuttgart, adelphi consult GmbH, Becker Büttner Held PartGmbB, Prognos AG, 2024-06. URL: https://www.kww-halle.de/praxis-kommunale-waermewende/bundesgesetz-zur-waermeplanung, last accessed: 2026-03-19.

[33] Bundesministerium für Wohnen, Stadtentwicklung und Bauwesen (BMWSB), ÖKOBAUDAT - Informationsportal Nachhaltiges Bauen - Version 2024-I, Berlin, Germany, 2024. URL: https://www.oekobaudat.de/, last accessed: 2026-03-19.

[34] WAMAK, s.r.o., Characteristic maps for commercial heat pumps, 2025. URL: https://wamak.eu/de/, last accessed: 2026-03-19.

[35] Carrier, AquaForce - Fixed-speed water-cooled screw liquid chiller 30XW / 30XW-P, 2025. URL: https://www.carrier.com/commercial/en/eu/products/air-conditioning/water-cooled-chillers/30xw-30xw-p/, last accessed: 2026-03-19.

[36] Institute for Automation and Applied Informatics (IAI), Karlsruhe Institute of Technology (KIT), KIT IFC examples, 2021. URL: https://www.ifcwiki.org/index.php?title=KIT_IFC_Examples, last accessed: 2026-03-19.